Role of Interparticle Charge Transfers in Agglomerated Photocatalyst Nanoparticles: Demonstration in Aqueous Suspension of Dye-Sensitized TiO2

ARTICLE *in* JOURNAL OF PHYSICAL CHEMISTRY LETTERS · DECEMBER 2012

Impact Factor: 7.46 · DOI: 10.1021/jz301881d

THE JOURNAL OF PHYSICAL CHEMISTRY Letters

Letter

pubs.acs.org/JPCL

Role of Interparticle Charge Transfers in Agglomerated Photocatalyst Nanoparticles: Demonstration in Aqueous Suspension of Dye-Sensitized TiO_2

Yiseul Park,[†,§] Wooyul Kim,[†] Damián Monllor-Satoca,[†] Takashi Tachikawa,[‡] Tetsuro Majima,[‡] and Wonyong Choi*[,†]

[†]School of Environmental Science and Engineering, Pohang University of Science and Technology (POSTECH), Pohang, 790-784, Korea

[‡]The Institute of Scientific and Industrial Research (SANKEN), Osaka University, Mihogaoka 8-1, Ibaraki, Osaka 567-0047, Japan

Supporting Information

ABSTRACT: The interparticle charge transfer within the agglomerates of TiO_2 nanoparticles in slurries markedly enhanced the dye-sensitized production of H_2 under visible light. By purposely decoupling the light absorbing part of Dye/TiO_2 from the active catalytic center of Pt/TiO_2, the role of bare TiO_2 nanoparticles working as a mediator that connects the above two parts in the agglomerates was investigated systematically. The presence of mediator in the agglomerate facilitated the charge separation and the electron transfer from Dye/TiO_2 to Pt/TiO_2 through multiple grain boundaries and subsequently produced more hydrogen. The dye-sensitized reduction of Cr(VI) to Cr(III) was also enhanced when Dye/TiO_2 nanoparticles were agglomerated with bare TiO_2 nanoparticles. The charge recombination between the oxidized dye and the injected electron was retarded in the presence of bare TiO_2 nanoparticles, and this retarded recombination on Dye/TiO_2 was confirmed by using transient laser spectroscopy. This phenomenon can be rationalized in terms of an interparticle Fermi level gradient within the agglomerates, which drives the charge separation.

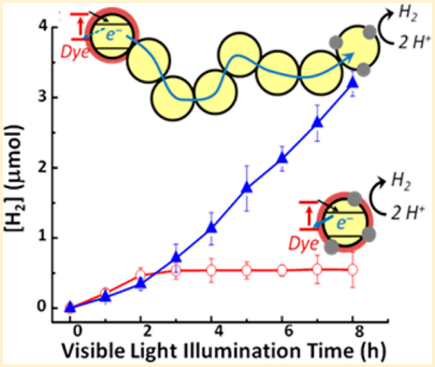

SECTION: Surfaces, Interfaces, Porous Materials, and Catalysis

Titanium dioxide-based photoactive materials find diverse applications, especially as a photocatalyst.[1]

Various parameters affecting their photocatalytic properties include particle size, crystalline phase, lattice or surface defects, surface area, and morphology of TiO_2.[2] Whereas these parameters are related mainly to the properties of individual particles, the role of the interparticle contact has been recognized as an additional parameter that influences the photoinduced charge-transfer processes in dye-sensitized solar cells (DSSCs) and photocatalysts.[3−12] In DSSC, $TiCl_4$ post-treatment of nanoporous thin films has been extensively used to improve the connectivity among TiO_2 nanoparticles with increasing the solar conversion efficiency.[3−6] In photocatalysis, it was observed that mesoporous TiO_2 consisting of densely packed nanoparticles (i.e., agglomerates) enhanced the photocatalytic activity for hydrogen production because the photogenerated charge pairs can be efficiently separated through the interparticle charge transfer within the agglomerates.[7−10] Likewise, TiO_2 fibers consisting of closely packed nanoparticles exhibited better photocatalytic activity than TiO_2 nanoparticles because of the efficient charge separation through interparticle charge transfer along the nanofiber framework.[11] Hartmann et al. reported that TiO_2 electrode composed of sol−gel-derived smaller particles showed better photocurrent generation than that with larger particles.[12] It seems that more continuous TiO_2 network with smaller particles leads to higher conduction of charge carriers within TiO_2 electrode. Szeifert et al. proposed the concept of "brick and mortar" by mixing the crystalline TiO_2 nanoparticles (bricks) with sol−gel titania (mortar).[13] For both NO oxidation and DSSC electrodes, mixtures with about 60−80% particle content exhibited the highest efficiencies. The benefit of mixture is attributed to good interconnection of particles via the sol−gel titania. The photoinduced charge transfers occurring on isolated nanoparticles seem to be different from those on the agglomerates of nanoparticles because the transfer and separation of photogenerated charge pairs are influenced by whether they are confined within a single particle or delocalized over the connected nanoparticles through the particle grain boundary.

The interparticle charge transfer in titania photocatalysis has been systematically studied by Bahnemann and coworkers,[14−20] who proposed the so-called "antenna mechanism" defined as the energetic coupling throughout a long chain of TiO_2 nanoparticles that enables energy or charge-carrier transfer

Received: November 18, 2012
Accepted: December 19, 2012

   dx.doi.org/10.1021/jz301881d | J. Phys. Chem. Lett. 2013, 4, 189−194

from a particle where the initial photon absorption takes place to another particle where the charge transfer finally occurs.[14,15] This may take place in all photocatalytic systems, including aggregated nanoparticles and nanocrystalline thin films. The physical and energetic interconnection among TiO_2 nanoparticles ensures an enhanced charge separation and a reduced recombination, which increases the charge carrier diffusion length.[17] The interconnection among nanoparticles should be different between the nanoparticle agglomerates in slurries and the nanoparticulate thin films. In this sense, Lana-Villarreal et al.[21,22] proved that the electron delocalization and charge carrier diffusion length were enhanced in nanoparticulate thin films of TiO_2 and WO_3 in comparison with those in the slurries of TiO_2 and WO_3. This mechanism has been repeatedly invoked in the literature for justifying the observed results, such as the oxidation of methanol with Fe(III)-doped titania,[14] mesoporous Au-TiO_2,[17] and Pd-TiO_2,[18] the hydrogen production,[8,9,20] and the degradation of dichloroacetic acid (DCA)[19] with Pt-TiO_2. Egerton et al.[23] recently reported that the photocatalytic degradation of DCA on Pt-TiO_2 was significantly retarded as the time of mechanical milling of catalyst powder increased. This could be ascribed to shattering the titania aggregates and breaking the titania−titania contact, which should reduce the efficiency of interparticle electron transfer.

Despite the numerous antenna phenomena evidence, the mechanism itself has not been appropriately tested. Most related experiments were carried out under UV irradiation, exciting all TiO_2 particles at once. Therefore, it is uncertain whether a real antenna effect prevails or not, and one could not clearly demonstrate whether the light absorbing particle and the charge-transferring particle are different. This study aimed to test the hypothesis of the antenna mechanism by isolating two components of the photocatalytic system (Scheme 1): one is the light-absorbing part of dye-sensitized TiO_2 nanoparticles (Dye/TiO_2) and the other is the TiO_2 nanoparticles loaded with the active center of Pt (Pt/TiO_2). Then, we added bare TiO_2 nanoparticles as a mediator that connect the above two parts and monitored how the presence of mediator TiO_2 influences the photocatalytic activity. The dye-sensitized production of H_2 under visible light was used as a main probe reaction: light is absorbed only by Dye/TiO_2, whereas hydrogen is generated only on Pt/TiO_2. Among the mixture aggregates of three different kinds of TiO_2 nanoparticles in the colloidal solution, the role of bare TiO_2 as a mediator can be investigated systematically and should be related to the interparticle charge transfer. The presence of bare TiO_2 (mediator) clearly influenced the electron-transfer process between Dye/TiO_2 and Pt/TiO_2, which was investigated by using both the photocatalytic reactivity test and the transient laser spectroscopy.

Scheme 1. Illustration of TiO_2 Nanoparticles Aggregate Assembly Employed for the Dye-Sensitized Production of H_2[a]

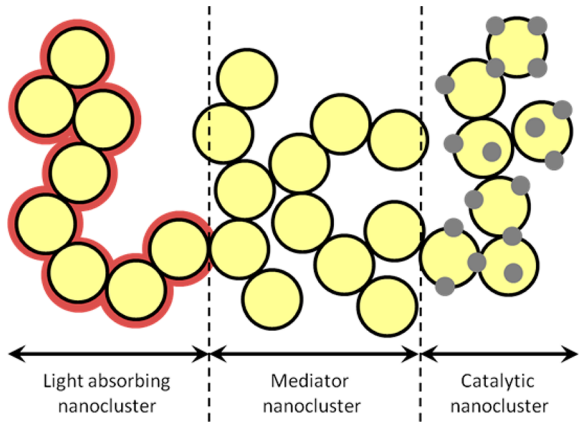

[a]Aggregates consist of three parts: (i) TiO_2 nanoparticles adsorbed with dye layer (red) that absorbs visible light, (ii) mediator nanocluster of bare TiO_2, and (iii) TiO_2 nanocluster with Pt cocatalyst (grey) on which H_2 is evolved. This scheme should not be mistaken for a composite film made of three stacked layers. The aggregate should be a random mixture of three parts, and the above illustration simplifies a situation where the three parts are in contact within an aggregate.

The preparation of TiO_2 colloid, an organic dye (see Figure S1 in the Supporting Information for its chemical structure) used as a sensitizer of TiO_2, platinized TiO_2, and the experimental conditions and procedures is described in detail in the Supporting Information. The effects of bare TiO_2 sol addition on the (Dye/TiO_2 + Pt/TiO_2) system were investigated by monitoring the hydrogen evolution reaction (HER) under visible-light irradiation. Either Dye/TiO_2 or Pt/TiO_2 alone under visible-light irradiation did not generate H_2 at all. The overall photocatalytic activity (quantified in terms of H_2 production) was measured in the mixture suspension of Dye/TiO_2 and Pt/TiO_2 with and without the third component (bare TiO_2) as a mediator that connects Dye/TiO_2 to Pt/TiO_2 nanoparticles. The mediator (bare TiO_2) itself neither absorbs the visible photons nor generates H_2. As for HER, the photoactive part is the visible-light-absorbing dye-adsorbed TiO_2 (Dye/TiO_2), whereas the catalytic part is the Pt site on TiO_2 (Pt/TiO_2, Scheme 1). The original mixture colloid (Dye/TiO_2 + Pt/TiO_2 + bare TiO_2) was nearly transparent in a well-dispersed state (@ pH 2), and the formation of colloid agglomerates was induced by raising pH to 4 (visible turbidity appeared; see Figure S2 in the Supporting Information). The average hydrodynamic particle size of the colloidal mixture that was determined by electrophoretic light scattering increased drastically from 397 nm at pH 2 (initial transparent colloid) to 2.55 μm at pH 4 (after coagulation).

To systematically investigate the HER process in the aggregates, we designed three experimental cases: (i) **case A**, where the light absorbing and catalytic parts are on the same nanoparticle (Dye/TiO_2/Pt); (ii) **case B**, where either part is separated in different nanoparticles (Dye/TiO_2 + Pt/TiO_2); and (iii) **case C**, where bare TiO_2 is added to mediate between two active parts (Dye/TiO_2 + TiO_2 + Pt/TiO_2). In all three cases, EDTA was used as an electron donor to regenerate the oxidized dyes. Although it has been previously reported that the surface complex of EDTA/TiO_2 has some visible-light activity for H_2 production,[24] the hydrogen production under the control experimental condition revealed that the visible activity of EDTA/TiO_2 complex was negligibly small. The time profiles of dye-sensitized hydrogen evolution among cases A, B, and C are compared in Figure 1a: the hydrogen production increased in the order of **case A** < **B** < **C**. The fact that **case B** showed a higher activity than **case A** implies that the electrons injected from the excited dyes (on one TiO_2 particle) are transferred to another Pt/TiO_2 particle through the particle boundary. Once electrons are separated from the oxidized dyes between different particles, the charge recombination should be more retarded than that in **case A**, where the electrons and the oxidized dyes are copresent on the same particle. This tendency

dx.doi.org/10.1021/jz301881d | J. Phys. Chem. Lett. 2013, 4, 189−194

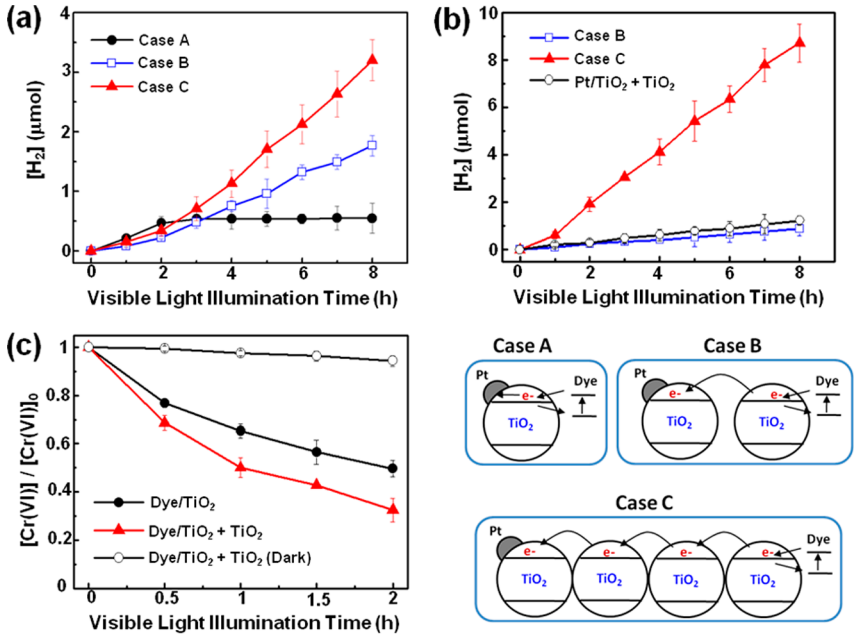

Figure 1. (a,b) Visible-light-induced production of hydrogen in the aqueous suspension of dye-sensitized TiO_2 nanoparticles among **Cases A**, **B**, and **C**. (a) Consisting of TiO_2 sol only. Experimental conditions: **Case A**, $[Dye/TiO_2/Pt] = 0.25$ g/L; **Case B**, $[Dye/TiO_2] = [Pt/TiO_2] = 0.25$ g/L; **Case C**, $[Dye/TiO_2] = [Pt/TiO_2] = [TiO_2] = 0.25$ g/L. (b) Consisting of commercial TiO_2 particles (P25) and TiO_2 sol. Experimental conditions: **Case B**, $[Dye/P25] = [Pt/TiO_2(sol)] = 0.25$ g/L; **Case C**, $[Dye/P25] = [Pt/TiO_2(sol)] = 0.25$ g/L; $[TiO_2(sol)] = 3$ g/L. In all cases, the amounts of active components (dye and Pt) in the reactor were the same. [EDTA] = 10 mM, $pH_i = 4.0$, $\lambda > 420$ nm. (c) Photoreduction of Cr(VI) to Cr(III) with TiO_2(sol). The concentration at time zero indicates the equilibrium concentration after chromium(VI) adsorption on the catalyst surface for 30 min. Experimental conditions: $[Dye/TiO_2] = [TiO_2] = 0.25$ g/L, $[Cr(VI)]_0 = 0.2$ mM, $pH_i = 4.0$, $\lambda > 420$ nm.

should be more marked with nanosized TiO_2 particle (than bulk-sized TiO_2) because the band bending for the efficient charge separation is not enough due to its limited size.[25] The hindered recombination should be responsible for the higher activity of **case B** than **case A**. The highest activity observed in **case C** can be explained in the similar way. The presence of mediator (bare TiO_2) in the aggregates facilitates the charge separation between Dye/TiO_2 and Pt/TiO_2 through multiple particle grain boundaries. The charge recombination in **case C** should be more hindered than in **case B** because bare TiO_2 nanoparticles intervene between dye/TiO_2 and Pt/TiO_2 nanoparticles (although some should be in direct contact as in **case B**).

A similar phenomenon was shown in Figure 1b when a commercial TiO_2 sample (Degussa P25) that has the state of highly agglomerated nanoparticles was employed as the substrate of dye sensitization (Dye/P25). Figure 1b compares the cases B and C that consist of Dye/P25, Pt/TiO_2(sol), and bare TiO_2(sol). **Case A** cannot be accurately represented when using P25, of which nanoparticles are already agglomerated: loading dye and Pt on the same nanoparticle among the agglomerates cannot be controlled. **Case C** exhibited a highly enhanced activity compared with **Case B** because bare TiO_2 sol successfully connects Dye/P25 and Pt/TiO_2(sol) upon agglomerating at pH 4.

The dye-sensitized conversion of Cr(VI) to Cr(III) was also tested as an alternative probe reaction to investigate the agglomeration effect in the $(Dye/TiO_2 + TiO_2)$ system (see Figure 1c). In this case, Pt/TiO_2 was not employed because the presence of Pt cocatalyst is not essentially needed for the reduction of Cr(VI). Although the reduction of Cr(VI) can occur on Dye/TiO_2 under visible-light irradiation, the addition of bare TiO_2 sol enhanced the removal rate of Cr(VI) as in the case of HER. This reconfirms that the charge separation between Dye/TiO_2 and adjacent bare TiO_2 nanoparticles in the agglomerates is facilitated through the interparticle boundaries to enhance the overall photocatalysis. Therefore, the fact that the photocatalysis on Dye/TiO_2 nanoparticles is enhanced upon agglomeration is demonstrated for both HER and the reduction of Cr(VI).

The role of bare TiO_2 in the sensitized production of hydrogen could be further confirmed by varying the concentration of bare TiO_2 , as shown in Figure 2. The overall

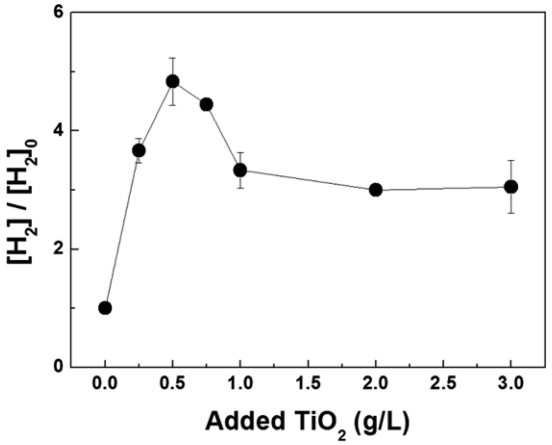

Figure 2. Dye-sensitized production of hydrogen in **Case C** (after 8 h of irradiation) as a function of mediator (bare TiO_2) concentration. The hydrogen amount in **Case C** ($[H_2]$) is represented on a relative scale against that generated in the absence of bare TiO_2 (i.e., **Case B**, $[H_2]_0$). Experimental conditions: $[Dye/TiO_2] = [Pt/TiO_2] = 0.25$ g/L, [EDTA] = 10 mM, $pH_i = 4.0$, and $\lambda > 420$ nm.

dx.doi.org/10.1021/jz301881d | J. Phys. Chem. Lett. 2013, 4, 189−194

photocatalytic activity was maximal at [bare TiO_2] = 0.5 g/L, above which the activity was reduced. This implies that there is an optimal size of agglomerate. The light shielding effect can be significant when the agglomerates are large enough to scatter incident light. The present results clearly support the fact that the separation of charge carriers generated on a Dye/TiO_2 nanoparticle and the subsequent interfacial charge transfer should be facilitated when there are adjacent TiO_2 nanoparticles by transferring electrons from one particle to another through the interparticle boundaries.

The charge recombination and interparticle electron transfer between Dye/TiO_2 and bare TiO_2 nanoparticles in the visible-light-irradiated suspension was further investigated by using time-resolved laser spectroscopy: the nonaggregated state (transparent sol) was probed by TAS, and the aggregated state (turbid suspension) was probed by transient diffuse reflectance spectroscopy (TDRS). The experimental setup is described in the Supporting Information and elsewhere.[26−28] The transient absorption decay of the photogenerated dye cation ($Dye^{\bullet+}$) on TiO_2 was compared in the absence and presence of bare TiO_2 in the nonaggregated (Figure 3a, by TAS) and aggregated (Figure 3b, by TDRS) states. The aggregation state of TiO_2 sol could be controlled simply by changing pH from 2 to 4. As shown in Figure 3, the addition of bare TiO_2 sol did not significantly change the transient absorption (dye cation) decay rate in the nonaggregated (transparent) state (Figure 3a), but considerably retarded its decay in the aggregated (turbid) state (Figure 3b). Upon adding bare TiO_2 sol to Dye/TiO_2 dispersion, the average lifetime (τ) of the dye cation increased from 4.9 to 8.4 μs (~2-fold increase) and from 6.7 to 120 μs (~18-fold increase) in the nonaggregated and aggregated state, respectively (see Table S1, Supporting Information). This clearly indicates that the close contact between Dye/TiO_2 and bare TiO_2 nanoparticles in the agglomerated state facilitates the interparticle electron transfer with retarding the back electron transfer (or charge recombination) from the TiO_2 conduction band to the adsorbed dye cation. Hence, the lifetime of the dye cation adsorbed on TiO_2 is prolonged when the nanoparticles are aggregated.

The interparticle charge-transfer process can be rationalized by proposing a 1-D nanoparticles chain model that simplifies the agglomerate behavior (Scheme 2). In the model, the first particle is a Dye/TiO_2, the last one is either a Pt/TiO_2 (for hydrogen production case) or a bare TiO_2 (for Cr(VI) reduction case), and the rest are bare TiO_2 nanoparticles (mediator). Once the first particle absorbs visible photons, electrons from the excited dyes are injected into TiO_2 CB, shifting its Fermi level ($E_{F,dye}$) toward more negative potential values. As a result, a Fermi level gradient is developed between the Dye/TiO_2 nanoparticle and the first mediator nanoparticle ($\Delta E_F = E_{F,1} - E_{F,dye}$) that drives an electron flux from the excited particle to the next unexcited one, where $E_{F,1}$ is the Fermi level of the first mediator nanoparticle.[29] This first interparticle charge transfer will set off a cascade of charge transfers until the electron reaches the final chain particle; hence, the electron transfer from the first to the last nanoparticle will be governed by their Fermi level gradient

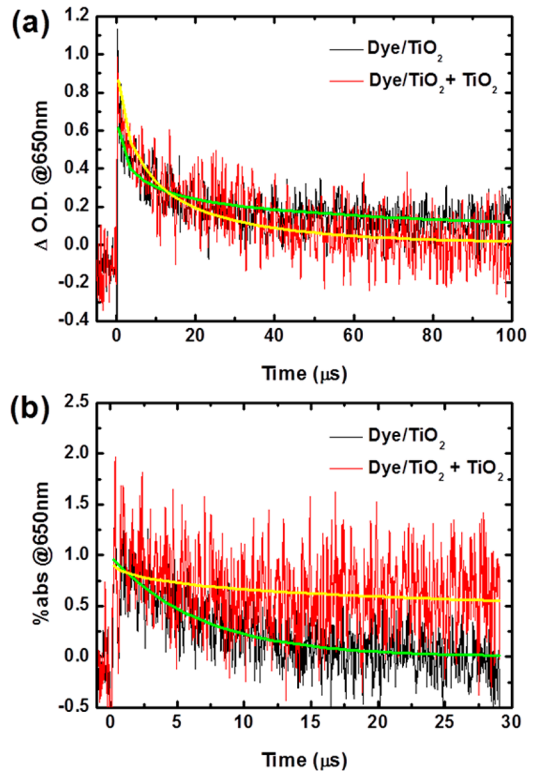

Figure 3. Normalized time traces of absorption at 650 nm ($Dye^{\bullet+}$) during the 532 nm laser photolysis (1.5 mJ $pulse^{-1}$) of Dye/TiO_2 (black line, without bare TiO_2) and [Dye/TiO_2 + bare TiO_2] (red line) in (a) nonaggregated colloid (at pH 2) and (b) aggregated state (at pH 4). Other experimental conditions were: [Dye/TiO_2] = [bare TiO_2] = 10 g/L, $[Dye]_0$ = 0.1 mM. The ordinate scale is %abs = $(R_0 - R)/R_0 \times 100$, where R_0 and R represent the intensities of the diffuse reflected monitor light before and after laser excitation, respectively. Green (Dye/TiO_2) and yellow (Dye/TiO_2 + bare TiO_2) lines represent the transient fittings with a stretched exponential function (see the fitting details in Table S1, Supporting Information).

Scheme 2. Illustration of a 1-D Chain (length, L) of N Nanoparticles (diameter, d) and the Variation of the Interparticle Fermi Level (ΔE_F), for the Hydrogen Evolution Process[a]

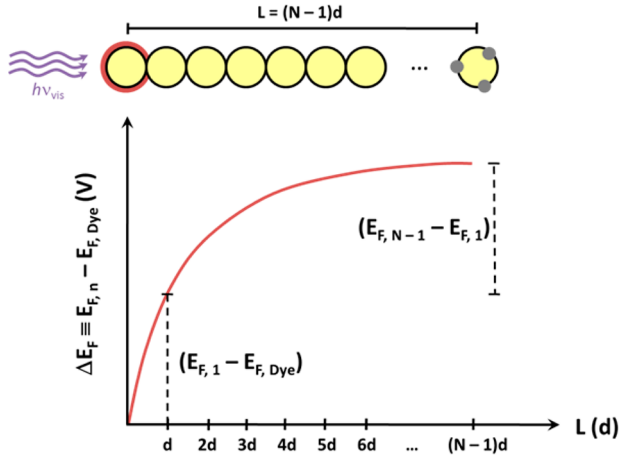

[a]Ordinate scale (ΔE_F) is defined as the difference between the Femi level of the nth particle ($E_{F,n}$) and that of the dye-adsorbed particle ($E_{F,dye}$). The dashed lines represent the Fermi level gradients between the first adjacent and the dye-adsorbed particle ($E_{F,1} - E_{F,dye}$), and the gradient between the last particle (Pt/TiO_2) and the first adjacent particle ($E_{F,N-1} - E_{F,1}$). The curve shape of the Fermi level gradient is only an illustration for qualitative description.

dx.doi.org/10.1021/jz301881d | J. Phys. Chem. Lett. 2013, 4, 189−194

($E_{F,n} - E_{F,1}$), where $E_{F,n}$ is the Fermi level of the nth mediator nanoparticle. The larger the initial gradient, the higher the probability of charge transfer to distant nanoparticles in the chain.[29] However, it should be noted that the above 1-D chain model is just an oversimplification, as the real behavior of the agglomerated nanoparticle clusters will be a 3D-averaged disordered charge-transfer phenomenon, similar to the stochastic random walk model for nanoporous thin films in DSSCs;[30] the energetic driving force of the real system could be similarly described by the previous model. Although the 1-D model should be regarded as a very rough approximation, the net electron transfer should be the same as in the 3-D electron transfer: from Dye/TiO_2 to Pt/TiO_2 according to the Fermi level gradient in the nanoparticle agglomerate.

In summary, we investigated the interparticle charge transfer in the agglomerates of nanoparticles, which consist of Dye/TiO_2, Pt/TiO_2, and bare TiO_2, and found that the presence of bare TiO_2 as a mediator that connects Dye/TiO_2 and Pt/TiO_2 nanoparticles markedly enhanced the dye-sensitized production of hydrogen by facilitating the charge separation through multiple grain boundaries within the agglomerates. The charge recombination between the oxidized dye and the injected electron was retarded when bare TiO_2 nanoparticles were additionally included within the aggregates, which was confirmed by using transient laser spectroscopy. On the basis of the present results, we can confirm that the nanoparticles in the agglomerates are closely coupled through the multiple particle boundaries and support "the antenna mechanism". Therefore, the photoexcitation site and the photocatalytic site can be spatially remote, and the degree of coupling between the remote sites should depend on how they are connected through "inert" mediator nanoparticles. This phenomenon could be operative when there is a substantial Fermi level gradient between the light-absorbing and catalytic nanoparticles. Further work is required to get a deeper insight into the real interparticle charge-transfer mechanism.

■ ASSOCIATED CONTENT

Supporting Information

Detailed experimental procedures, chemical structure of the organic dye (Figure S1), turbidity change of the TiO_2 slurries upon aggregation at pH 4 (Figure S2), and fitting details of the transient spectra decays (Table S1). This material is available free of charge via the Internet at http://pubs.acs.org.

■ AUTHOR INFORMATION

Corresponding Author

*Fax: +82-54-279-8299. E-mail: wchoi@postech.edu.

Present Address

[§]Department of Chemistry, University of Wisconsin-Madison, Madison, WI 53705, USA

Notes

The authors declare no competing financial interest.

■ ACKNOWLEDGMENTS

This work was supported by KOSEF NRL program (no. R0A-2008-000-20068-0), the KOSEF EPB center (grant no. R11-2008-052-02002), the Global Frontier R&D Program on Center for Multiscale Energy System (2011-0031571), and KCAP (Sogang Univ.) funded by MEST through NRF (NRF-2011-C1AAA001-2011-0030278). The organic dye used in this study was kindly provided by Prof. S. O. Kang of Korea University.

■ REFERENCES

(1) Fujishima, A.; Zhang, X.; Tryk, D. A. TiO_2 Photocatalysis and Related Surface Phenomena. *Surf. Sci. Rep.* **2008**, *63*, 515−582.

(2) Prieto-Mahaney, O. O.; Murakami, N.; Abe, R.; Ohtani, B. Correlation Between Photocatalytic Activities and Structural and Physical Properties of Titanium (IV) Oxide Powders. *Chem. Lett.* **2009**, *38*, 238−239.

(3) O'Regan, B. C.; Durrant, J. R.; Sommeling, P. M.; Bakker, N. J. Influence of the $TiCl_4$ Treatment on Nanocrystalline TiO_2 Films in Dye-Sensitized Solar Cells. 2. Charge Density, Band Edge Shifts, and Quantification of Recombination Losses at Short Circuit. *J. Phys. Chem. C* **2007**, *111*, 14001−14010.

(4) Yu, H.; Zhang, S.; Zhao, H.; Will, G.; Liu, P. An Efficient and Low-Cost TiO_2 Compact Layer for Performance Improvement of Dye-Sensitized Solar Cells. *Electrochim. Acta* **2009**, *54*, 1319−1324.

(5) Yu, H.; Zhang, S.; Zhao, H.; Xue, B.; Liu, P.; Will, G. High-Performance TiO_2 Photoanode with an Efficient Electron Transport Network for Dye-Sensitized Solar Cells. *J. Phys. Chem. C* **2009**, *113*, 16277−16282.

(6) Yu, H.; Zhang, S.; Zhao, H.; Zhang, H. Photoelectrochemical Quantification of Electron Transport Resistance of TiO_2 Photoanodes for Dye-Sensitized Solar Cells. *Phys. Chem. Chem. Phys.* **2010**, *12*, 6625−6631.

(7) Lakshminarasimhan, N.; Bae, E.; Choi, W. Enhanced Photocatalytic Production of H_2 on Mesoporous TiO_2 Prepared by Template-Free Method: Role of Interparticle Charge Transfer. *J. Phys. Chem. C* **2007**, *111*, 15244−15250.

(8) Lakshminarasimhan, N.; Kim, W.; Choi, W. Effect of the Agglomerated State on the Photocatalytic Hydrogen Production with In Situ Agglomeration of Colloidal TiO_2 Nanoparticles. *J. Phys. Chem. C* **2008**, *112*, 20451−20457.

(9) Lakshminarasimhan, N.; Bokare, A. D.; Choi, W. Effect of Agglomerated State in Mesoporous TiO_2 on the Morphology of Photodeposited Pt and Photocatalytic Activity. *J. Phys. Chem. C* **2012**, *116*, 17531−17539.

(10) Bian, Z.; Tachikawa, T.; Majima, T. Superstructure of TiO_2 Crystalline Nanoparticles Yields Effective Conduction Pathways for Photogenerated Charges. *J. Phys. Chem. Lett.* **2012**, *3*, 1422−1427.

(11) Choi, S. K.; Kim, S.; Lim, S. K.; Park, H. Photocatalytic Comparison of TiO_2 Nanoparticles and Electrospun TiO_2 Nanofibers: Effects of Mesoporosity and Interparticle Charge Transfer. *J. Phys. Chem. C* **2010**, *114*, 16475−16480.

(12) Hartmann, P.; Lee, D.-K.; Smarsly, B. M.; Janek, J. Mesoporous TiO_2: Comparison of Classical Sol-Gel and Nanoparticle Based Photoelectrodes for the Water Splitting Reaction. *ACS Nano* **2010**, *4*, 3147−3154.

(13) Szeifert, J. M.; Fattakhova-Rohlfing, D.; Georgiadou, D.; Kalousek, V.; Rathouský, J.; Kuang, D.; Wenger, S.; Zakeeruddin, S. M.; Grätzel, M.; Bein, T. "Brick and Mortar" Strategy for the Formation of Highly Crystalline Mesoporous Titania Films from Nanocrystalline Building Blocks. *Chem. Mater.* **2009**, *21*, 1260−1265.

(14) Wang, C.-Y.; Bottcher, C.; Bahnemann, D. W.; Dohrmann, J. K. A Comparative Study of Nanometer Sized Fe(III)-Doped TiO_2 Photocatalysis: Synthesis, Characterization and Activity. *J. Mater. Chem.* **2003**, *13*, 2322−2329.

(15) Wang, C.-Y.; Pagel, R.; Dohrmann, J. K.; Bahnemann, D. W. Antenna Mechanism and Deaggregation Concept: Novel Mechanistic Principles for Photocatalysis. *C. R. Chim.* **2006**, *9*, 761−773.

(16) Zhang, H.; Chen, G.; Bahnemann, D. W. Photoelectrocatalytic Materials for Environmental Applications. *J. Mater. Chem.* **2009**, *19*, 5089−5121.

(17) Ismail, A. A.; Bahnemann, D. W. Nanocomposites as Highly Active Photocatalysts for the Photooxidation of Dichloroacetic Acid. *J. Phys. Chem. C* **2011**, *115*, 5784−5791.

(18) Ismail, A. A.; Bahnemann, D. W.; Bannat, I.; Wark, M. Gold Nanoparticles on Mesoporous Interparticle Networks of Titanium

Dioxide Nanocrystals for Enhanced Photonic Efficiencies. *J. Phys. Chem. C* **2009**, *113*, 7429−7435.
(19) Ismail, A. A.; Bahnemann, D. W.; Robben, L.; Yarovyi, V.; Wark, M. Palladium Doped Porous Titania Photocatalysts: Impact of Mesoporous Order and Crystallinity. *Chem. Mater.* **2010**, *22*, 108−116.
(20) Kandiel, T. A.; Dillert, R.; Robben, L.; Bahnemann, D. W. Photonic Efficiency and Mechanism of Photocatalytic Molecular Hydrogen Production over Platinized Titanium Dioxide from Aqueous Methanol Solutions. *Catal. Today* **2011**, *161*, 196−201.
(21) Lana-Villarreal, T.; Monllor-Satoca, D.; Gómez, R.; Salvador, P. Determination of Electron Diffusion Lengths in Nanostructured Oxide Electrodes From Photopotential Maps Obtained with the Scanning Microscope for Semiconductor Characterization. *Electrochem. Commun.* **2006**, *8*, 1784−1790.
(22) Lana-Villarreal, T.; Monllor-Satoca, D.; Rodes, A.; Gómez, R. Photocatalytic Behavior of Suspended and Supported Semiconductor Particles in Aqueous Media: Fundamental Aspects using Catechol as Model Molecule. *Catal. Today* **2007**, *129*, 86−95.
(23) Egerton, T. A.; Mattinson, J. A. Effects of Particle Dispersion on Photocatalysis Probed by The Effect of Platinum on Dichloroacetic Acid Oxidation by P25 and Nanoparticulate Rutile. *Appl. Catal., B* **2010**, *99*, 407−412.
(24) Kim, G.; Choi, W. Charge-Transfer Surface Complex of EDTA-TiO_2 and Its Effect on Photocatalysis under Visible Light. *Appl. Catal., B* **2010**, *100*, 77−83.
(25) Liqiang, J.; Xiaojun, S.; Jing, S.; Weimin, C.; Zili, X.; Yaoguo, D.; Honggang, F. Review of Surface Photovoltage Spectra of Nano-Sized Semiconductor and Its Applications in Heterogeneous Photocatalysis. *Sol. Energy Mater Sol. Cells* **2003**, *79*, 133−151.
(26) Vinodgopal, K.; Hua, X.; Dahlgren, R. L.; Lappin, A. G.; Patterson, L. K.; Kamat, P. V. Photochemistry of $Ru(bpy)_2(dcbpy)^{2+}$ on $A1_2O_3$ and TiO_2 Surfaces. An Insight into the Mechanism of Photosensitization. *J. Phys. Chem.* **1995**, *99*, 10883−10889.
(27) Kim, W.; Tachikawa, T.; Majima, T.; Choi, W. Photocatalysis of Dye-Sensitized TiO_2 Nanoparticles with Thin Overcoat of Al_2O_3: Enhanced Activity for H_2 Production and Dechlorination of CCl_4. *J. Phys. Chem. C* **2009**, *113*, 10603−10609.
(28) Kim, W.; Tachikawa, T.; Majima, T.; Li, C.; Kim, H.-J.; Choi, W. Tin-Porphyrin Sensitized TiO_2 for the Production of H_2 under Visible Light. *Energy Environ. Sci.* **2010**, *3*, 1789−1795.
(29) Berger, T.; Monllor-Satoca, D.; Jankulovska, M.; Lana-Villarreal, T.; Gómez, R. The Electrochemistry of Nanostructured Titanium Dioxide Electrodes. *Chem. Phys. Chem.* **2012**, *13*, 2824−2875.
(30) Anta, J. A.; Mora-Sero, I.; Dittrich, T.; Bisquert, J. Dynamics of Charge Separation and Trap-Limited Electron Transport in TiO_2 Nanostructures. *J. Phys. Chem. C* **2007**, *111*, 13997−14000.